Influence of wafer thickness on the performance of multicrystalline Si solar cells; an experimental study

C.J.J. Tool, A.R. Burgers, P. Manshanden, A.W. Weeber
ECN Solar Energy, PO Box 1, 1755 ZG Petten, The Netherlands

B.H.M. van Straaten
Shell Solar Energy B.V., PO Box 849, 5700 AV Helmond, The Netherlands

The influence of the thickness of silicon solar cells has been investigated using neighbouring multicrystalline silicon wafers with thickness ranging from 150 to 325 µm. For silicon solar cell structures with a high minority carrier diffusion length one expects that J_{sc} would decrease as the wafer becomes thinner due to a shorter optical path length. It was found experimentally that J_{sc} is nearly independent of the thickness of the solar cell, even when the minority carrier diffusion length is about 300 µm. This indicates that the Al rear metallisation acts as a good back surface reflector. A decrease in J_{sc} is observed only if the wafer thickness becomes less than about 200 µm.

The observed trend in V_{oc} as a function of the wafer thickness has been explained with PC1D modelling by a minority carrier diffusion length in the Al-doped BSF which is small in relation to the thickness of the BSF. This effectively increases the recombination velocity at the rear of the cell.

We have shown that the efficiency of solar cells made with standard industrial processing is hardly reduced by reducing the wafer thickness. Solar cell efficiencies might be increased by better rear surface passivation.

Keywords: photovoltaics; wafer thickness; lifetime; BSF; multicrystalline silicon; PC1D modelling

Introduction

It is generally accepted that the cost of photovoltaic conversion has to diminish for PV to become of major importance as a renewable energy source.[1] For crystalline silicon wafer technology, the silicon material is a major cost item.[2] One option to make a more efficient use of the expensive silicon material is the use of thinner silicon wafers. The total amount of silicon used per Wp decreases by about 20 % when using 200 µm wafers instead of 300 µm wafers in spite of relatively increased kerf losses when process yield and cell efficiency are not affected.

Within the present investigation we studied the influence of the wafer thickness of both high quality and low quality base material on the electrical properties of the mc-Si solar cells. The material quality of the cells has been varied by using different processing schemes.

Thus far, experimental studies on the influence of wafer thickness on cell efficiency have been hampered by the absence of neighbour wafers with varying thickness. Interpretation of the results was thus complicated because of possible differences in (electronic) material quality of wafers with different thickness. Now experiments have been performed on multicrystalline silicon neighbour wafers with varying thickness.

The significance of the influence of the wafer thickness on the solar cell characteristics was investigated using statistical analysis. Solar cell results have been modelled with PC1D.

Experimental set-up

Sets of silicon wafers have been processed using standard processing sequences using industrial techniques (see Figure 1). Each set consisted initially of eight 10×10 cm^2 neighbour wafers. The thickness of the 8 wafers before the saw damage etch ranged from 150 µm to 325 µm with steps of 25 µm. Because of breakage of cells either during wafer fabrication, handling or cell processing, several sets consisted of less than 8 cells. Two different scenarios have been used to process the wafers into solar cells, the main difference being the emitter sheet resistance and the anti reflection coating (ARC). A thick emitter in combination with a TiO_2 ARC resulted in solar cells with a relatively short minority carrier diffusion length. A shallow emitter in combination with a passivation SiN_x ARC should result in solar cells with a much longer minority carrier diffusion length due to passivation by the SiN_x. Throughout this article, the TiO_2 scenario refers to the low material quality scenario, while the SiN_x scenario refers to the high material quality scenario.

The SiN_x ARC was applied with a remote microwave plasma enhanced CVD (R-MW-PECVD) system[3] at ECN, the TiO_2 coating was applied with an industrial atmospheric pressure CVD (APCVD) system at Shell Solar Energy B.V.. A total of 22 neighbour sets has been processed; 10 with an SiN_x ARC and 12 with a TiO_2 ARC (see Table 1).

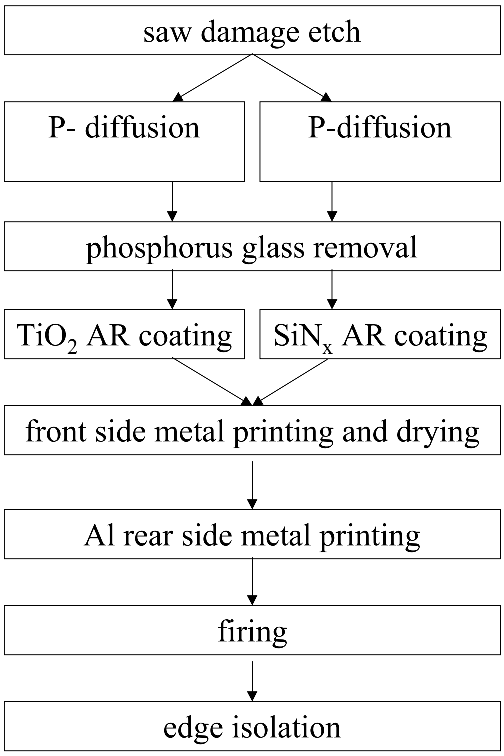

Figure 1: Applied process sequence; firing conditions used were different for the different scenarios and varied slightly with wafer thickness. The firing conditions were not fully optimised for each thickness.

Table 1: Variations in the neighbour sets used.

group	wafer thickness	AR coating	# neighbour sets
A	150 – 325 μm	SiN_x	10
B	150 – 325 μm	TiO_2	12

We assume that the improvement of the bulk material quality by SiN_x is independent of the wafer thickness. Only then the neighbour wafers still have comparable material quality after processing. A set of 330 μm neighbour wafers and a set of 200 μm neighbour wafers have been processed with both SiN_x and TiO_2 ARC to validate this assumption.

To determine the internal reflection at the aluminium rear metallisation, a measured reflection curve of a specially prepared sample was modelled using a stratified system with scattering surfaces. The scattering is modelled using the Phong model.[4]

We measured the IV characteristics of all cells. The reflectance, the spectral response and the ECV-profile of the BSF of selected cells was measured. The statistical analysis to identify significant trends has been performed using the program Statgraphics version 5[+]. The device modelling was done with PC1D version 4.5[5]. Although this is a one-dimensional model, the observed trends of the various cell parameters are expected to be comparable to a more complicated two-dimensional model.

Method of statistical analysis

Weeber and Sinke have shown the importance of the use of a two factor analysis of variance to determine whether or not observed trends are significant, specially when neighbour wafers are used[6]. In this work one of the factors is the thickness, the other factor is the neighbour type (statistical block). We want to investigate whether or not the cell results (J_{sc}, V_{oc}, FF) depend on the thickness of the cell.

The cell result of an individual cell can be represented by:

$$y_{ij} = \mu + \tau_i + \beta_j + \varepsilon_{ij} \qquad 1$$

in which:

- i = thickness indicator (1, 2, ….a) (i = 1 for 150 μm, i = 8 for 325 μm wafers)
- j = neighbour set (1, 2, …b) (b = 12 for TiO_2; b = 10 for SiN_x)
- y_{ij} = individual cell result (J_{sc}, V_{oc}, FF)
- μ = the overall mean
- τ_i = the effect of the thickness
- β_j = the effect of neighbour set j
- ε_{ij} = the usual random error term

The effect of the thickness and the effect of the neighbour set are defined as deviations from the overall mean. The sum of the squares SS can be split in a term of the thickness, a term of the neighbour set and an error term:

$$SS_T = SS_{thickness} + SS_{neighbour} + SS_{error} \qquad (2)$$

The mean square of the thickness ($MS_{thickness}$) indicates the variability of the thickness and $MS_{neighbour}$ indicates the variability within the neighbour solar cells. MS_{error} indicates the variability of the random error term. Table 2 shows the formulae to calculate the mean squares .

Table 2: Analysis of variance for a complete block design

source of variation	degrees of freedom	mean square
thickness	a-1	$\frac{SS_{thickness}}{a-1}$
neighbours	b-1	$\frac{SS_{neighbour}}{b-1}$
error	(a-1)(b-1)	$\frac{SS_{error}}{(a-1)(b-1)}$
total	ab-1	

The observed difference between two thicknesses is significant if the difference between the means of the two thicknesses is greater then the *least significant difference* LSD. In formula form:

$$\left|\bar{y}_{i.} - \bar{y}_{k.}\right| > LSD \text{ with } LSD = t_{\alpha/2,(a-1)(b-1)}\sqrt{2MS_{error}/b} \qquad (3)$$

$t_{\alpha/2,((a-1)(b-1)}$ is a statistical factor (t-statistics) and depends on the confidence limit (95% in our case) and the degrees of freedom. The value of t can be found in standard books on statistics. Note that MS_{error} not only depends on the variance of the solar cells with thickness i and k, but also on the variance of all the solar cells. MS_{error} is also used to calculate the confidence limits in Table 3 to Table 5. The confidence limit is not the standard deviation within the group, but is calculated as $\pm\, t_{\alpha/2,ab-a}\sqrt{MS_{error}/b}$.

A more detailed discussion of the statistical method is given by Montgomery[7]. In our case the calculations are complicated because values are missing. During wafer production and cell processing wafers are broken; more breakage occurred for thinner wafers. The method to compensate for those missing values is described by Montgomery[7] in chapter 5.

We used the computer program Statgraphics[8] to perform the calculations.

Results

To investigate the significance of observed trends, the main electrical parameters have been analysed statistically. Throughout this discussion, the 95 % confidence limit is used to identify significant differences. In Table 3 and Table 4 the mean value of the main electrical parameters of the groups are given.

In Table 3 the mean values of the main electrical parameters of the solar cells processed according to the SiN_x scenario are given (group A). Within the 95 % confidence limit, both J_{sc} and V_{oc} are independent of the wafer thickness, as long as the wafer thickness is over 200 µm. If thinner wafers are used, the decrease in both V_{oc} and J_{sc} becomes statistically significant.

Table 3: Cell results of neighbour cells with varying thickness processed with an SiN_x ARC (group A). Errors show 95 % confidence limit.

thickness µm	J_{sc} mA/cm^2	V_{oc} mV	FF %	η %
325	30.2 ± 0.2	601 ± 2	74.4 ± 0.9	13.5 ± 0.2
300	29.8 ± 0.2	601 ± 2	74.1 ± 0.9	13.3 ± 0.2
275	30.2 ± 0.2	602 ± 2	73.4 ± 0.8	13.3 ± 0.2
250	30.0 ± 0.2	601 ± 2	74.2 ± 0.9	13.4 ± 0.2
225	29.9 ± 0.2	602 ± 2	74.6 ± 0.8	13.4 ± 0.2
200	29.7 ± 0.2	600 ± 2	74.7 ± 0.8	13.3 ± 0.2
175	29.3 ± 0.2	599 ± 2	73.4 ± 1.0	12.9 ± 0.2
150	29.1 ± 0.2	597 ± 3	71.4 ± 1.3	12.4 ± 0.2

In Table 4 the mean values of the main electrical parameters for the solar cells processed following the TiO_2 scenario are given (group B). The statistical analysis shows that both J_{sc} and V_{oc} are independent of the wafer thickness within the 95 % confidence limit.

Table 4: Cell results of neighbour cells with varying thickness processed with an TiO_2 ARC (group B). Errors show 95 % confidence limit.

thickness µm	J_{sc} mA/cm^2	V_{oc} mV	FF %	η %
325	26.3 ± 0.1	581 ± 2	70.3 ± 0.5	10.8 ± 0.2
300	26.5 ± 0.2	582 ± 2	72.0 ± 0.5	11.1 ± 0.2
275	26.6 ± 0.1	582 ± 2	72.6 ± 0.5	11.2 ± 0.2
250	26.3 ± 0.2	581 ± 2	73.8 ± 0.5	11.3 ± 0.2
225	26.6 ± 0.2	582 ± 2	73.1 ± 0.5	11.3 ± 0.2
200	26.7 ± 0.2	582 ± 2	73.2 ± 0.5	11.3 ± 0.2
175	26.7 ± 0.2	581 ± 3	72.5 ± 0.8	11.3 ± 0.2
150	26.8 ± 0.5	583 ± 6	73.1 ± 1.6	11.4 ± 0.2

The results of the experiments to validate the assumption the bulk passivation is independent of the wafer thickness and the experiments to estimate the internal rear reflectivity do not directly contribute to the insight in the influence of the wafer thickness on the solar cell performance in relation to the material quality. For that reason the results are discussed in this section and not in the discussion section.

SiN_x bulk passivation in thick and thin wafers

In Table 5 the mean values of the main electrical parameters of neighbour cells processed according to the two different scenarios are given. For the 330 and 200 µm thick neighbours both V_{oc} and J_{sc} are significantly higher for the SiN_x scenario compared to the TiO_2 scenario. This is in accordance with results reported by Duerinckx et al.[9].

Table 5: Cell results of neighbour cells with the same thickness processed using different scenarios. Errors show 95 % confidence limit.

scenario	thickness µm	J_{sc} mA/cm^2	V_{oc} mV	FF %	η %
TiO_2	330	28.1 ± 0.2	598 ± 1	71 ± 1	11.9 ± 0.2
SiN_x	330	30.4 ± 0.2	609 ± 1	72 ± 1	13.3 ± 0.2
TiO_2	200	27.2 ± 0.2	584 ± 2	73 ± 1	11.6 ± 0.1
SiN_x	200	29.9 ± 0.3	604 ± 3	73 ± 1	13.2 ± 0.2

In Figure 2 the IQE data for 330 µm thick cells processed using the SiN_x and TiO_2 scenario respectively are shown. Neighbour wafers have been used for this experiment, so differences in materials properties of the starting wafers can be neglected. The IQE in the SiN_x scenario is higher for all wavelengths.

The increase in blue response results from the shallower emitter in the SiN_x scenario in combination with some surface passivation. The increase in red response results from the bulk passivating properties of the SiN_x ARC reported before[3]. Using PC1D modelling, the minority carrier diffusion length for the SiN_x scenario and the TiO_2 scenario were estimated at 400 µm and 200 µm, respectively (curve marked “calculated”)

In Figure 3 the measured and calculated IQE data for the 200 µm thick neighbour wafers are shown. Again, the differences can be attributed to differences in emitter profile and the surface and bulk passivation by the SiN_x ARC. As for the 330 µm thick wafers, a large improvement in minority carrier diffusion length is observed for the SiN_x scenario.

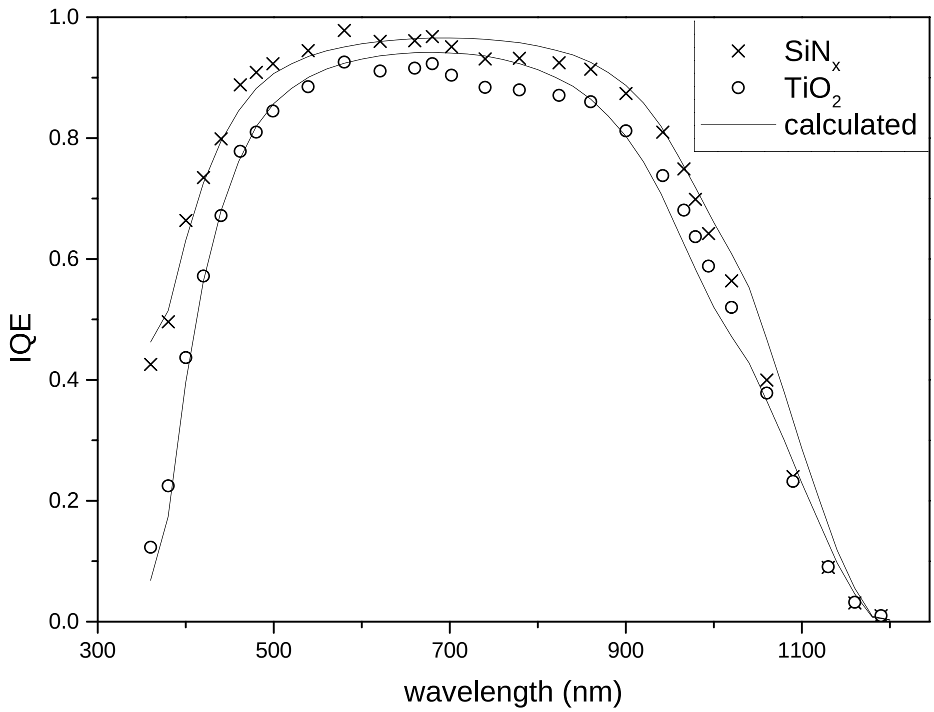

Figure 2: Internal Quantum Efficiency for 330 µm thick neighbour cells; SiN_x and TiO_2 scenario respectively. Solid lines are calculated with PC1D using minority carrier diffusion lengths of 400 and 200 µm resp.

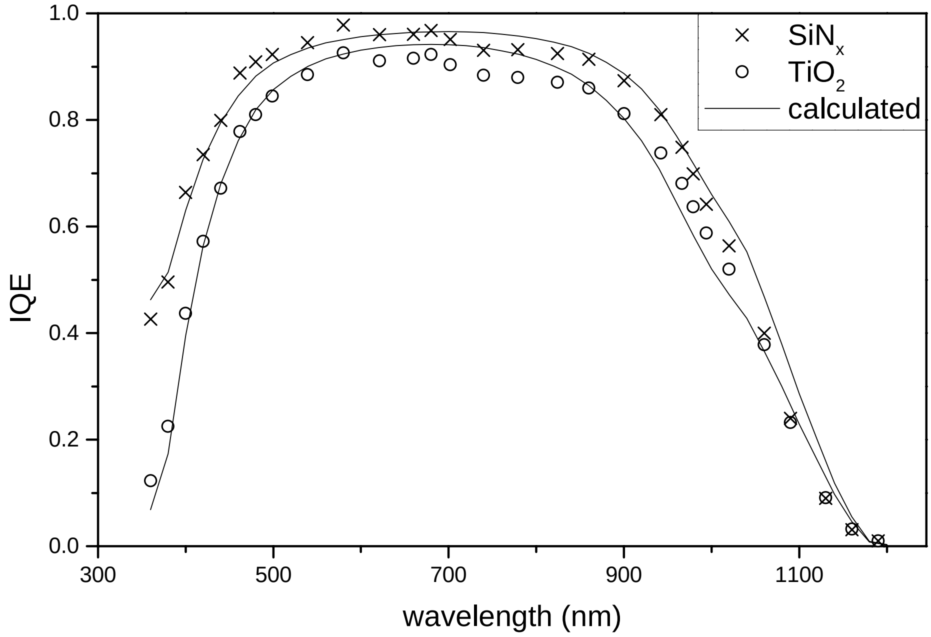

Figure 3: Internal Quantum Efficiency for 200 µm thick neighbour cells; SiN_x and TiO_2 scenario resp. Solid lines are calculated with PC1D using minority carrier diffusion lengths of 350 and 150 µm resp.

For both wafer thicknessess the minority carrier diffusion length is increased by about 200 µm. This indicates that the increase in material quality by the SiN_x ARC is independent of the wafer thickness. Neighbour wafers thus still have identical material quality after the SiN_x processing sequence and the SiN_x ARC is useable to investigate the influence of the wafer thickness on neighbour wafers with a (relatively) high (induced) material quality. The TiO_2 scenario is used to obtain results on (relatively) poor material quality.

N.B. note that the 330 µm wafers and the 200 µm wafers are not neighbours of each other.

Rear side reflectivity

In order to estimate the internal reflection coefficient of the rear side, screen printed aluminium BSF were made on 50 µm thick mono crystalline double polished wafers using different firing conditions. The reflection curves were measured and subsequently modelled using the Phong model. This model allows to adjust the scattering continuously from perfectly specular to perfectly Lambertian. Phong coefficient and reflection coefficient are intimately coupled. For instance if the rear surface is supposed to be specular, the reflection coefficient must be low, otherwise the modelled reflection will be too high. However, changing the Phong coefficient also changes the optical path length. So the correct pair of Phong coefficient and reflection coefficient can be found by comparison of the calculated and measured reflection in the region were silicon is semitransparent (950 to 1100 nm). This allows to pinpoint the optical properties of the BSF accurately. This model has been used by us in the past to model the optical properties of saw-damage etched multi-crystalline silicon wafers.[10]

The Phong coefficient and the reflection coefficient of the Al rear were supposed to be wavelength independent over the wavelength region of interest. In Figure 4 the results of the modelling is shown. We observe that assuming a more scattering rear surface results in a shift of the sloping part of the calculated reflection curve to higher wavelengths (see insert). The difference between measured and the calculated reflection curve is minimal if an internal reflection coefficient at the rear Al surface of 78 % is assumed. The reflection is mainly diffuse with a Phong coefficient of about 2.0 (see Table 6). The rear side reflection was found to be nearly independent (± 1 %) of the firing conditions.

Table 6: Phong and reflection pairs used in modelling.

Phong constant	reflection
4.2	73 %
3.4	75 %
2.5	77 %
2	78 %
1.5	79 %
0.5	80 %

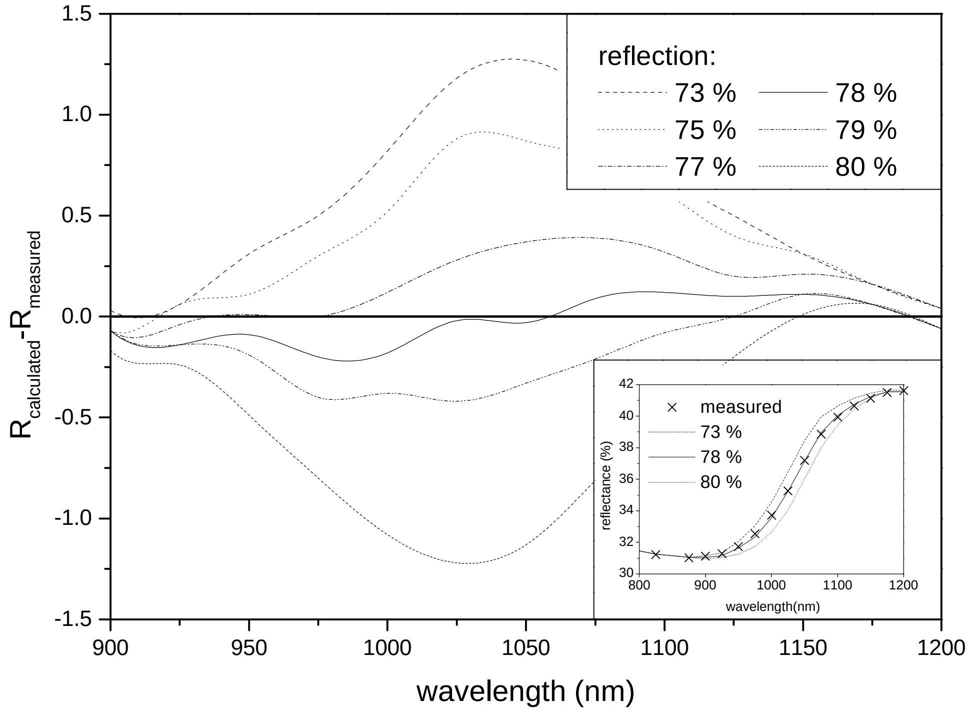

Figure 4: Difference between calculated and measured external reflection for various internal reflectances at the aluminium rear. Insert shows the shift to higher wavelengths if the internal rear reflection increases.

Discussion

Wafer thickness and material quality effect on short circuit current J_{sc}.

We investigated for both high and low quality base material the influence of the wafer thickness on the solar cell characteristics. In both scenarios V_{oc} and J_{sc} are independent of the wafer thickness for most thicknesses. Only for wafer thickness less than 200 µm in the SiN_x scenario a statistically significant decrease in the short circuit current is observed. The independence of J_{sc} can be explained by the high reflectivity of the aluminium rear metallisation shown above (see Figure 4). For the thinnest wafers in the SiN_x scenario, the reflectivity is too low to prevent some loss in J_{sc}.

In Figure 5 the measured and calculated short circuit current for both scenarios are shown. The statistical analysis for the TiO_2 scenario indicates that J_{sc} is independent of the wafer thickness. However, Figure 5 suggests that in this scenario the spreading in the short circuit current decreases with decreasing wafer thickness. Particularly the lower short circuit currents seem to disappear. This trend has been observed before in large scale experiments also (unpublished results). This can be qualitatively explained by the high internal reflectivity combined with a low effective bulk diffusion length. Due to the low bulk diffusion length, electrons generated near the rear side of the solar cell have a very low probability for collection. Due to the high internal rear reflection, the total generation is hardly reduced by thinning the wafer. But the generation takes place closer to the junction and that will increase the collection probability.

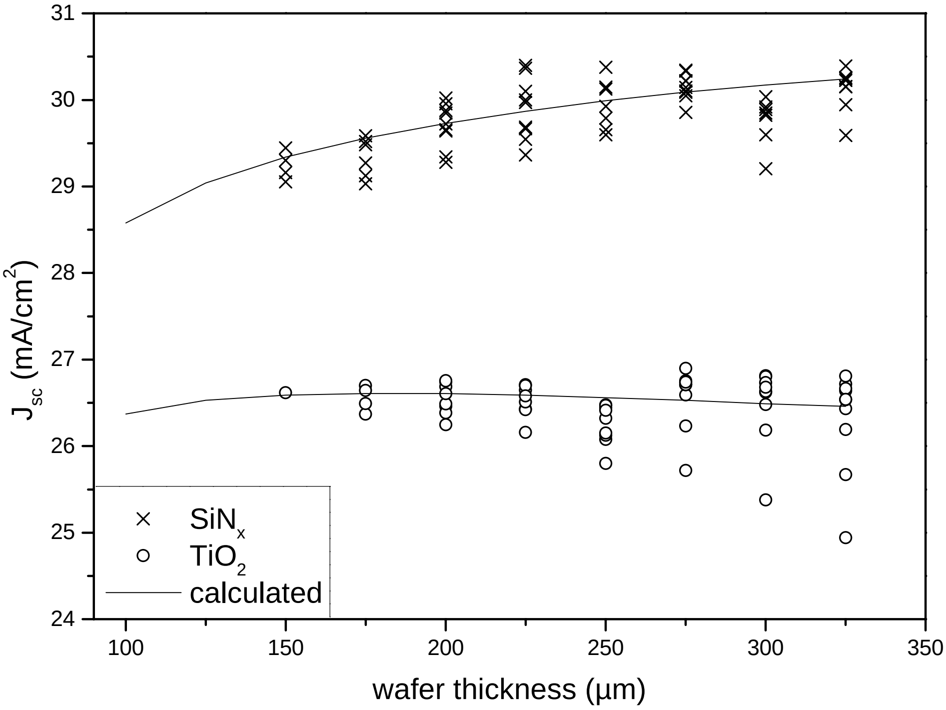

Figure 5: Scatterplot of J_{sc} as a function of the wafer thickness for both scenarios. Solid curves calculated using PC1D; SiN_x: L_{bulk} = 350 µm, L_{BSF} = 0.3 µm, S_{front} = $1.5 \cdot 10^5$ cm/s, TiO_2: L_{bulk} = 100 µm, L_{BSF} = 0.35 µm, S_{front} = 10^7 cm/s.

Wafer thickness and material quality effect on open circuit voltage V_{oc}.

The independence of V_{oc} on the wafer thickness results from the relative low quality of the aluminium BSF. V_{oc} is a function of the temperature T, the light generated current J_L (ideally this is equal to J_{sc}) and the dark saturation current J_0:

$$V_{oc} = \frac{kT}{q} \ln\left(\frac{J_L}{J_0} + 1 \right) \tag{4}$$

The dark saturation current of a silicon device depends on the effective recombination velocities. The contribution of the base to the dark saturation current is given by [11]:

$$J_{0p} = \frac{qD_p n_i^2}{L_p N_a} * F_p \tag{5}$$

With:

$$F_p = \frac{S_p \cosh\left(\frac{W_p}{L_p}\right) + \frac{D_p}{L_p} \sinh\left(\frac{W_p}{L_p}\right)}{\frac{D_p}{L_p} \cosh\left(\frac{W_p}{L_p}\right) + S_p \sinh\left(\frac{W_p}{L_p}\right)} \tag{6}$$

For devices having a BSF, the actual surface recombination velocity S_p has to be replaced by the effective recombination velocity S_{eff}. Instead of using the well known equation established by Godleski[12], we used S_{eff} estimated by PC1D because of the limitations of the Godleski model[13]. In equation (5), only F_p depends on the wafer thickness. From equation (6) it can be concluded that the influence of the wafer thickness is cancelled out in F_p and V_{oc} is thus independent of the wafer thickness if either:

$$\cosh\left(\frac{W_p}{L_p}\right) = \sinh\left(\frac{W_p}{L_p}\right) \quad \Rightarrow W_p >> L_p \tag{7}$$

or:

$$S_{eff} = \frac{D_p}{L_p} \tag{8}$$

Equation (7) is a general case, equation (8) is a coincidental condition which holds for only 1 value of the minority carrier diffusion length.

To investigate whether the independence of V_{oc} on the wafer thickness results from the bulk diffusion length (equation (7)) or the rear surface passivation (equation (8)), the experimental results have been modelled using PC1D. To obtain a starting point for the modelling of the neighbour solar cells, the minority carrier diffusion length in the bulk, the diffusion length in the BSF and the front surface recombination velocity has been modified by iteration until both the measured IQE, the J_{sc} and the V_{oc} are fitted well by PC1D for the 325 µm thick wafer. In this iteration process, some parameters were fixed on their measured experimental values (see Table 7).

Table 7: Experimental values used in PC1D calculations.

	SiN_x scenario	TiO_2 scenario	measured by
front metal coverage	9 %	9 %	visual inspection
emitter peak [P]	$1.0 \cdot 10^{23}$ at P / cc	$1.6 \cdot 10^{23}$ at P / cc	
emitter R_{sheet}	50 Ω.	40 Ω.	
emitter profile	error function	error function	
[B] base (=N_a)	$1 \cdot 10^{16}$ at B / cc	$1.2 \cdot 10^{16}$ at B/cc	ECV*
[B] BSF (=N_a^+)	$5 \cdot 10^{18}$ at B / cc	$2 \cdot 10^{18}$ at B/cc	ECV
thickness BSF	9 µm	5 µm	ECV
rear reflection	78 %	78 %	modelling (Figure 4)
refractive index ARC	2.2	2.3	reflection
thickness ARC	71 nm	73 nm	reflection
D_p	28.6 cm^2 / sec	28.0 cm^2 / sec	calculated from N_a

*: Electrochemical Capacitance/Voltage measurement. The base dopant concentration in the TiO_2 scenario is based on PC1D modelling. Note that the wafers used in the two scenarios are no neighbours of each other.

D_p is used to calculate equation (8)

In Figure 6 the measured and calculated IQE curves for the 325 µm thick wafer processed with the SiN_x scenario are shown. To obtain the best fit for this scenario, a minority carrier diffusion length of 350 µm had to be assumed. For the diffusion length in the BSF a value of 0.3 µm has been used and for the front surface recombination a velocity of $1.5.10^5$ cm/s had to be assumed. From PC1D modelling, this is equivalent with an effective rear side recombination velocity of 3500 cm/s. According to equation (8), V_{oc} would be independent of the thickness in this experiment if S_{eff} = 820 cm/s. For S_{eff} < 820 cm/s, V_{oc} would increase with increasing wafer thickness, for S_{eff} > 820 cm/s V_{oc} would decrease (see Figure 7). Also, $W_p < L_p$, so neither the condition of equation (7) nor the condition of equation (8) is fulfilled. Because $S_{eff} > 820$ cm/s, the modelling predicts that V_{oc} should decrease with decreasing wafer thickness.

In this work it is experimentally found that V_{oc} is independent of the wafer thickness for wafers thicker than 200 µm. This results from the sensitivity of V_{oc} to S_{eff} and the wafer thickness in the range of interest. In Figure 7 the sensitivity of V_{oc} to the effective rear surface recombination velocity in the SiN_x scenario is shown. The curves are calculated with PC1D, using the input parameters as given in Table 7. Instead of modelling a BSF, the rear surface recombination velocity is set at the value given in the legend. The figure shows that for S_{eff} = 3500 cm/s, V_{oc} decreases by about 6 mV for a 200 µm wafer compared to a 325 µm thick wafer. Due to the small amount of wafers the observed statistical variation in this experiment is no contradiction to the decrease predicted by the PC1D modelling. On large quantities a slight decrease in V_{oc} should be observed.

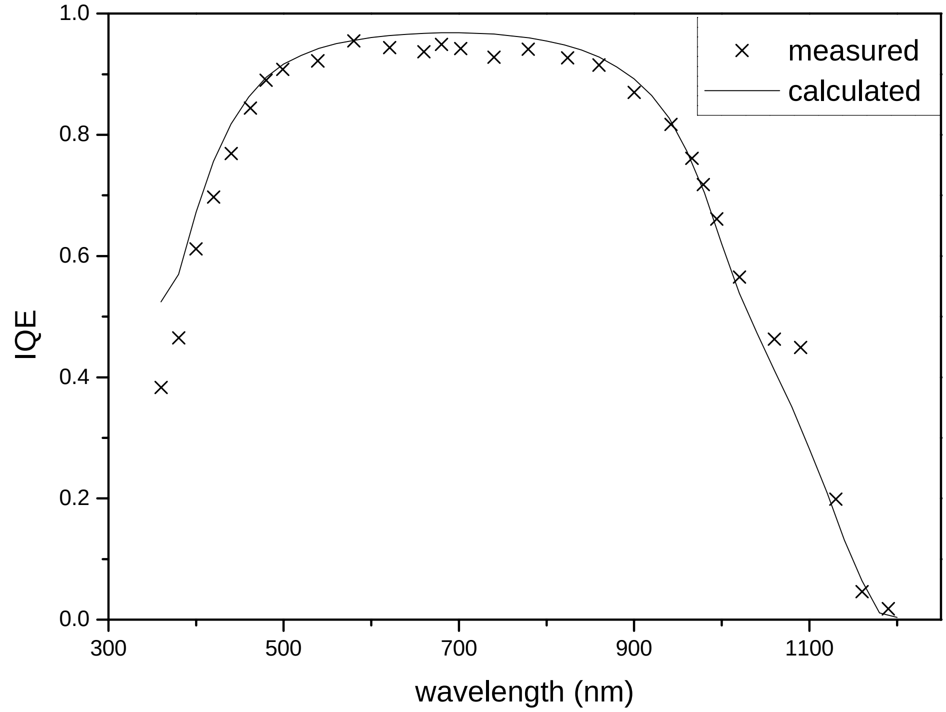

Figure 6: Internal Quantum Efficiency for 325 µm wafer with SiN_x scenario. Solid curve calculated using PC1D: L_{bulk} = 350 µm; L_{BSF} = 0.3 µm, $S_{front} = 1.5.10^5$ cm/s.

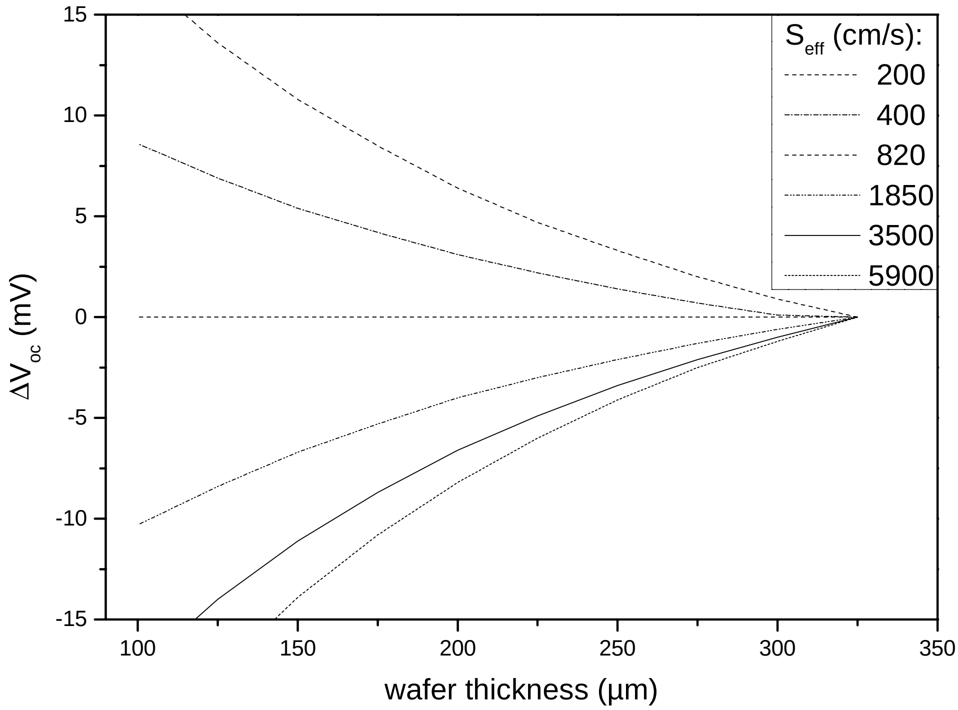

Figure 7: Calculated change in V_{oc} as a function of the wafer thickness for various effective rear side recombination velocities. A 325 µm thick wafer is taken as reference.

In Figure 8 the measured and calculated V_{oc} data for both scenarios are shown. For the high quality material (SiN_x) PC1D modelling predict a small decrease in V_{oc} with decreasing wafer thickness. However, as can bee seen in the figure, the magnitude of the decrease is within the experimental variations. This confirms that the dependence is not statistically significant in this experiment.

The best fit for the low quality material (TiO_2) has been obtained using a minority carrier diffusion length of 100 µm for the bulk and 0.35 µm for the BSF. The front surface recombination velocity was found to be 10^7 cm/s. In this scenario, the condition given by equation (7) ($L_p \ll W_p$) is fulfilled. The independence of the wafer thickness on the V_{oc} results from the low material quality of the wafers.

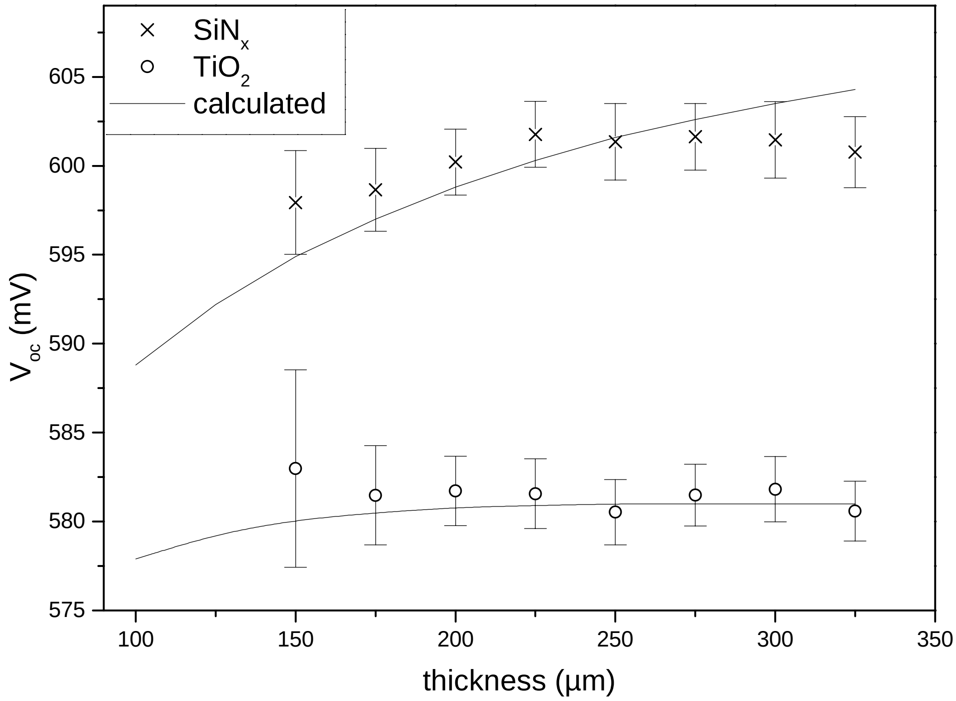

Figure 8: V_{oc} as a function of the wafer thickness for both scenarios. Error bars show 95 % confidence limits. Solid curve calculated using PC1D; SiN_x: L_{bulk} = 350 µm, L_{BSF} = 0.3 µm, S_{front} = $1.5 \cdot 10^5$ cm/s, TiO_2: L_{bulk} = 100 µm, L_{BSF} = 0.35 µm, S_{front} = 10^7 cm/s.

In Figure 9 the influence of the wafer thickness on V_{oc} for various material qualities and two rear surface passivation schemes is shown. For Si solar cells with an average rear surface passivation (S_{eff} = 3500 cm/s), a decrease in the wafer thickness results in a decrease of the V_{oc}. This decrease is biggest for cells with a good bulk quality. Because these cells normally have a higher V_{oc}, the modelling predicts that the use of thinner wafers will result in a smaller V_{oc} distribution.

For cells with a good rear surface passivation (e.g. S_{eff} < 200 cm/s) an increase in V_{oc} is predicted. For cells with a low material quality which normally have the lowest V_{oc}, the increase is less than for cells with a moderate or good material quality. The use of thinner wafers in combination with a good rear surface passivation scheme will broaden the V_{oc} distribution because the increase in V_{oc} is smallest for the wafers with the lowest V_{oc}.

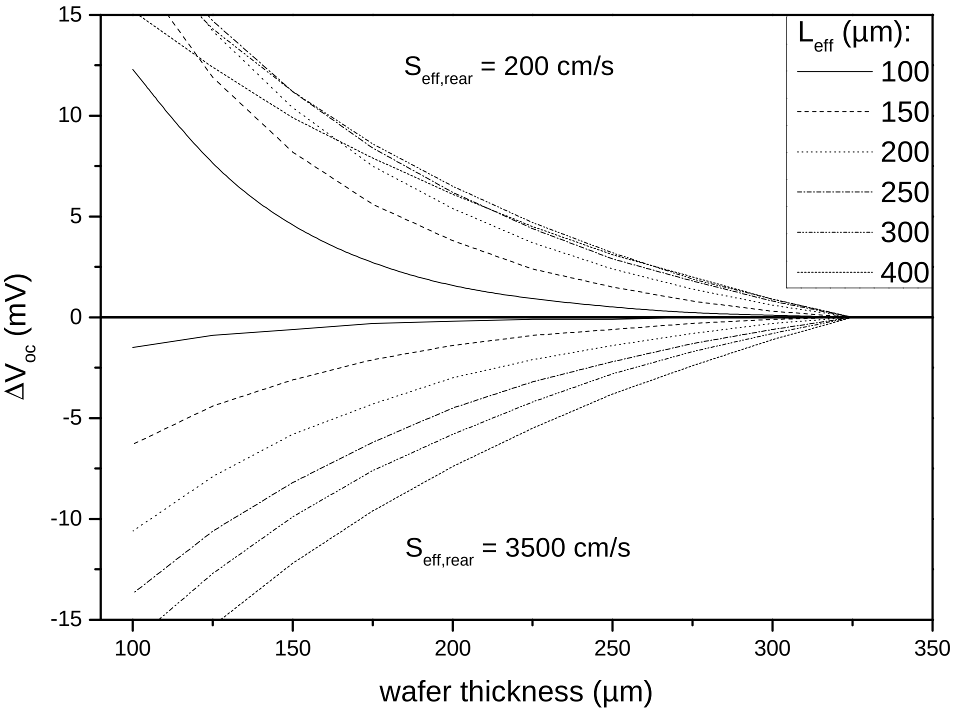

Figure 9: Influence of wafer thickness on V_{oc} for various material qualities for two rear surface passivation schemes.

The reason for the dramatically low diffusion length in the BSF is not yet fully understood. It may result from the quality of the aluminium that is used; it is known that the Al paste contains Fe contamination. Whether this is the main reason, or if stresses induced by the alloy process induce (additional) materials degradation needs further investigation.

Wafer thickness and material quality effect on efficiency.

The results indicate that for the presently used Al BSF rear side passivation scheme J_{sc} is independent of the wafer thickness for wafers thicker than 200 µm for both high and low quality material. The spreading in J_{sc} will probably decrease due to an expected increase in J_{sc} for very low quality material. Within experimental error a slight decrease in V_{oc} can be expected for the high quality material on an industrial scale, resulting in a slight decreased variation of V_{oc}.

In this work we observed a significant influence of the wafer thickness on the fill factor. However, in our opinion this is because the firing conditions used were not fully optimised for the various wafer thickness. We have no indications that the fill factor is influenced by the thickness assuming optimum firing conditions are used. Therefore the decreased variation in both J_{sc} and V_{oc} result in a smaller efficiency distribution for thinner wafers in large scale experiments where optical firing conditions will be used.

In Figure 10 the efficiency is shown as a function of the wafer thickness for both scenarios together with some PC1D calculations. To extract the influence of the fill factor on the efficiencies, a FF of 0.75 is used in this figure to calculate the efficiencies. The high recombination velocity is a limiting factor to the solar cell efficiency. As an example, the efficiencies are calculated assuming a rear side recombination velocity of only 200 cm/s. Such recombination velocities can be obtained using a well passivating SiN_x coating[14,15], a high quality highly doped Al BSF[16] or by using B-doped Al paste to increase the doping level of the alloy[17]. This would increase the efficiency of the high quality wafers by about 1 to 1.5 % absolute, the increase for the poor quality wafers would be negligible for the thick wafers and increase to about 0.5 % for the 150 µm thin wafers. The efficiency distribution would thus increase dramatically. This will probably mean that such rear surface passivating processing sequences must be combined with bulk passivating or gettering processing sequences in a production environment.

To obtain the indicated efficiency gains the high internal reflectance of the device has to be maintained.

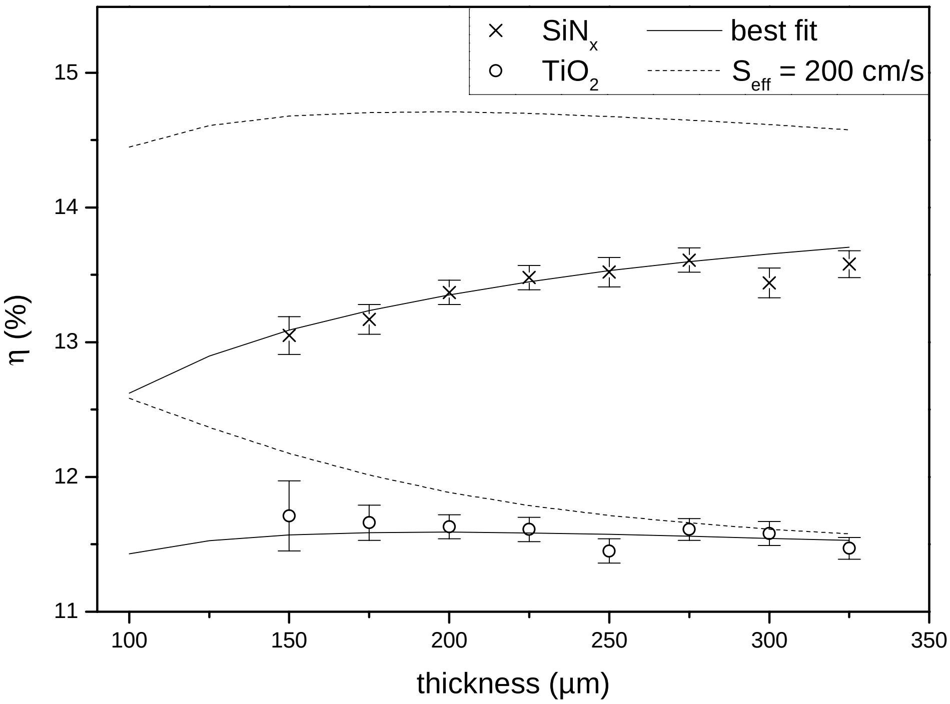

Figure 10: Influence of thickness on efficiency for various rear side passivation schemes on high (SiN_x) and low (TiO_2) quality material.

Conclusion

For both the high and low quality material, the efficiency of mc-Si solar cells is practically independent of the thickness for wafer thickness larger than 200 µm. For thinner wafers, the efficiency of the cells with a high bulk quality decreases while it is still constant for the cells with a low bulk quality. On a large quantity of cells, it is expected that a small significant decrease in V_{oc} will be observed. However, the V_{oc} distribution might be somewhat narrower. The low minority carrier diffusion length in the Al-BSF results in a high effective surface recombination velocity which prohibits the expected increase in the V_{oc} for thinner wafers.

The unexpected independence of J_{sc} on the wafer thickness is attributed to a high internal reflection at the rear side Al for the cells with a high quality material. Because of the internal reflection the current loss is minimised. For cells with a poor bulk quality, an increase in J_{sc} is expected, resulting in a narrower distribution in J_{sc} as for V_{oc}. The experimental results indicate that the need for additional light trapping only becomes important for wafer thickness less that 200 µm.

From this work it can be concluded that for the used back surface passivation scheme, the use of thinner wafers will not reduce the average solar cell efficiency. The efficiency distribution will be narrowed. This shows that, providing that the overall production yield is not reduced, thinner wafers can assist in lowering the cost of PV. PC1D calculations indicate that major improvements in solar cell performance can be realised if other rear surface passivation schemes are applied, but these schemes may result in a broadening of the efficiency distribution.

Acknowledgements

This work has been made possible by the financial support of the NOZ-PV programme from The Netherlands Agency for Energy and the Environment (Novem) and the Dutch Economy, Ecology and Technology programme, a joint initiative of the ministry of Economic Affairs, the ministry of Education, Culture and Science and the ministry of Public Housing, Physical Planning and Environment.

We thank Eric Kossen, Martien Koppes and Hans ter Beeke for their effort in the processing of the wafers, and Henk Rieffe and GertJan Langedijk for their prompt and accurate analysis of the solar cells. We also acknowledge Wim Sinke for the worthwhile discussions on the subject.

References

1. Groenendaal BJ, de Lange TK, Lako P, van Roosmalen JAM, Tool CJJ, de Wild-Scholten MJ. Critical succes factors for the large-scale introduction of grid-connected photovoltaic systems. report no ECN-C--00-086, 2000.
2. Frantzis L, Jones E, Lee C, Wood M, Wormser P. Opportunities for cost reductions in photovotaic modules. *Proceedings of the 16th European PV Solar Energy Conference* 2000; 2100-2103.
3. Soppe WJ, Duijvelaar BG, Schiermeier SEA, Weeber AW, Steiner A, Schuurmans FM. A high throughput PECVD reactor for deposition of passivating SiN layers. *Proceedings of the 16th European PV Solar Energy Conference* 2000; 1420-1423.
4. *Illumination and Color in Computer Generated Imagery.* Springer Verlag (1989).
5. Basore PA, Clugston DA. PC1D version 4 for windows: from analysis to design. *Proceedings of the 25th IEEE PV Specialist Conference* 1996; 377-381.
6. Weeber AW, Sinke WC. Statistical analysis for solar cell research. *Proceedings of the 25th IEEE PV Specialists Conference* 1996, 565-567.
7. Montgomery DC. *Design and analysis of experiments.* Wiley, New York, 1991, Chapter 3-5.
8. http://www.statgraphics.com September 2001.
9. Duerinckx F, Szlufcik J, de Clerq K, de Schepper P, Laureys W, Nijs J, Mertens R. PECVD silicon nitride passivation and ARC layers for screenprinted multicrystalline silicon solar cells. *Proceedings of the 13th European PV Solar Energy Conference* 1995; 1493-1496.
10. Burgers AR, Kinderman R, Hylton JD, Sinke WC, de Moor HHC. Light-trapping in saw-damage etched silicon wafers. *Proceedings of the 14th European PV Solar Energy Conference* 1997; 143-146.
11. Green MA. *Solar cells, Operating principles, technology and system applications*. University of New South Wales: Kensington, 1992; sect. 4.9.
12. Godlewski MP, Baraona CR, Brandhorst HW. Low-high junction theory applied to solar cells. *Proceedings of the 10th IEEE PV Specialist Conference* 1973; 40-43.
13. Kaminski A, Vandelle B, Boyeau JP, Laugier A, Monna R, Le Quan Nam, Sarti D. BSF analysis on multicrystalline silicon solar cells. *Proceedings of the 16th European PV Solar Energy Conference* 2000; 1267-1270.
14. Schuurmans FM, *Surface passivation of silicon by PECVD silicon nitride.* PhD Thesis: Utrecht University, 1998.
15. Aberle AG. Surface passivation of crystalline silicon solar cells: A review. *Progress in Photovoltaics: Research and Applications* 2000; **8**, 473-487.
16. Narasimha S, Rohatgi A, Weeber AW. An optimized rapid aluminium back surface field technique for silicon solar cells. *IEEE Trans Electron Devices* 1999; **46**(7), 1363

17. Lölgen P. *Surfance and volume recombination in silicon solar cells*. PhD Thesis: Utrecht University, 1995.